

# The IR sector of QCD: lattice versus Schwinger-Dyson equations

Daniele Binosi

*European Centre for Theoretical Studies in Nuclear Physics and Related Areas (ECT\*), Villa Tambosi, Strada delle Tabarelle 286, I-38050 Villazzano (TN), Italy*

**Abstract.** Important information about the infrared dynamics of QCD is encoded in the behavior of its (of-shell) Green's functions, most notably the gluon and the ghost propagators. Due to recent improvements in the quality of lattice data and the truncation schemes employed for the Schwinger-Dyson equations we have now reached a point where the interplay between these two non-perturbative tools can be most fruitful. In this talk several of the above points will be reviewed, with particular emphasis on the implications for the ghost sector, the non-perturbative effective charge of QCD, and the Kugo-Ojima function.

**Keywords:** Nonperturbative Effects, QCD

**PACS:** 12.38.Lg, 12.38.Aw, 12.38.Gc

## INTRODUCTION

Even though the Green's (correlation) functions of pure Yang-Mills theories are not *per se* physical objects (given that they depend explicitly on the gauge-fixing and renormalization scheme used), the discovery and understanding of their infrared (IR) properties has become an increasingly active topic. In fact, the prevailing opinion to date is that they represent crucial pieces in our effort to unravel the non-perturbative QCD dynamics and to fully understand confinement.

The exploration of the IR sector of Yang-Mills theories is currently pursued through mainly two non perturbative tools, namely the lattice – where space-time is discretized and the quantities of interest are evaluated numerically – and the Schwinger-Dyson equations – corresponding to the infinite set of integral equation governing the dynamics of the Green's functions.

Recent years have witnessed a lot of progress in both methods [1, 2], and it looks like we have come to a point in which it is meaningful to systematically compare SDE results with lattice predictions.

For the particular case of the gluon propagator and ghost dressing function, the solutions of the Landau gauge SDEs fall into two very distinct classes, namely:

- *Massive solutions* [3, 4]: These solutions show a gluon propagator and a ghost dressing function that saturate in the IR to a finite (and non-zero) value, in complete agreement with the mechanism of confinement through thick vortex condensation, proposed by Cornwall [5].
- *Scaling solutions* [6]: These solutions are characterized by power-law behavior with well-defined exponents, and lead to an IR vanishing gluon propagator and,

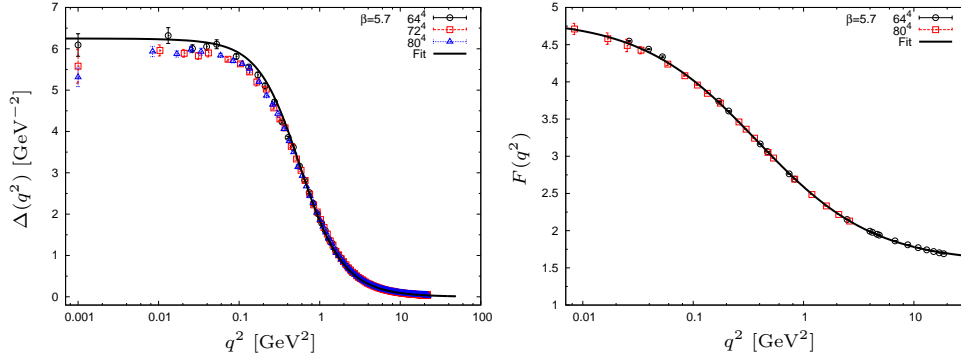


**FIGURE 1.** Lattice data for the SU(3) gluon propagator and ghost dressing function [9]. Solid lines corresponds to fits in terms of a massive gluon propagator and a finite ghost dressing function.

correspondingly, an IR diverging ghost dressing function; they are tailored to satisfy the confinement scenarios of Kugo-Ojima [7] and Gribov-Zwanziger [8].

Over the last few years, ab-initio lattice computations have been crucial in deciding which of these two types of solutions are in fact realized in (Landau gauge!) QCD. As a result, a consistent and clear picture has emerged that strongly advocates for the massive solutions. In Fig. 1 we show the lattice data for the Landau gauge SU(3) [9] gluon propagator and ghost dressing function. One can see the appearance of a plateau for the gluon propagator in the deep IR region (which is one of the most salient and distinctive predictions of the gluon mass generation mechanism), and no enhancement for the ghost dressing function in the deep IR, where instead, it again saturates to a constant. The lattice data can be in fact accurately fitted in terms of a massive gluon propagator and a finite ghost dressing function (see Fig. 1); indeed this is also valid for all lattice simulations available from different groups (e.g., for the SU(2) case [1, 10]).

Landau gauge lattice studies therefore seem to rule out the possibility of scaling solutions with nontrivial infrared exponents (and consequently the Kugo-Ojima scenario). It also disfavor the original formulation of the Gribov-Zwanziger scenario, though the drastic modifications brought in by the inclusion of dimension two condensates, reconcile it with the lattice results [11].

In what follows we will concentrate on the PT-BFM (pinch technique - background field method) framework [5, 12], where the aforementioned lattice findings may be naturally accommodated. In fact, the discovery of the key underlying ingredient, namely the dynamical generation of a gluon mass, coincided historically with the invention of the PT [5], long before any lattice simulations were even contemplated.

## PT-BFM EQUATIONS AND NUMERICAL RESULTS

**PT-BFM equations.** The application of the pinch technique [12] to the conventional gluon self-energy SDE, gives rise *dynamically* to a new SDE [2] (see Fig. 2), where (i) on the lhs the PT-BFM self-energy  $\widehat{\Pi}_{\mu\nu}$  appears, whereas (ii) on the rhs the graphs display the conventional self-energy  $\Pi_{\mu\nu}$  but are made out from BFM vertices which

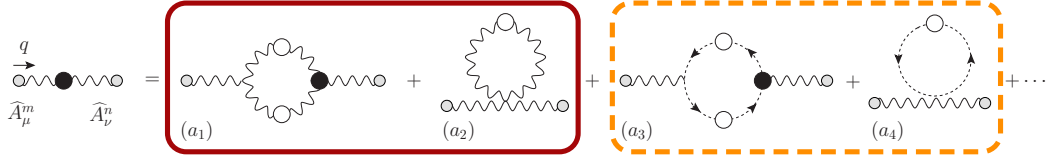


**FIGURE 2.** The block-wise transverse SDE for the gluon self-energy in the PT-BFM framework. The dots indicates that two-loop dressed gluon and ghost diagrams have been omitted.

satisfy simple Ward identities. This implies in turn that the new SDE is composed of one- and two-loop dressed gluon and ghost contributions which are individually transverse. The conventional and BFM self-energies are related through the identity [13]  $\Delta = [1 + G]^2 \hat{\Delta}$  where  $G$  is on of the form factors of a certain auxiliary function  $\Lambda_{\mu\nu} = g_{\mu\nu}G + (q_\mu q_\nu / q^2)L$ . Then considering only the one-loop dressed diagrams of Fig. 2 and tracing out the transverse projectors, one can write

$$\Delta^{-1}(q^2) = \frac{q^2 + i \sum_{i=1}^4 (a_i)}{[1 + G(q^2)]^2}. \quad (1)$$

We next express the background three gluon and ghost vertex appearing in diagrams  $(a_1)$  and  $(a_3)$  as a function of the gluon and ghost self-energies in such a way as to (i) automatically satisfy the Ward identities and (ii) to introduce the massless poles necessary to trigger the Schwinger mechanism [14]. The Ansatz we will use is

$$\tilde{\Gamma}_{\alpha\mu\nu} = \Gamma_{\alpha\mu\nu}^{(0)} + i \frac{q_\alpha}{q^2} [\Pi_{\mu\nu}(k+q) - \Pi_{\mu\nu}(k)], \quad (2)$$

and similarly for the ghost vertex  $\tilde{\Gamma}_\alpha$ . The resulting expression for the SDE (1) after projection to the Landau gauge is very lengthy [4]. The important point is that the resulting gluon self-energy is IR finite,  $\Delta^{-1}(0) > 0$ .

**Gluon and ghost Green's functions.** The solutions of the PT-BFM equations (1) SU(3) case [4] are shown in Fig. 3. The agreement found between the SDE and the lattice results allows one to study other quantities of interest by using the lattice directly as an input into the various SDE. The general strategy adopted in this case is the following. One takes the lattice gluon propagator as an input for the ghost SDE; then solves for the ghost dressing function, tuning the coupling constant  $g$  such that the solution gives the best possible approximation to the lattice result. Obviously one must check that the coupling so obtained (at the renormalization scale used for the computation) is fully consistent with known perturbative results (obtained in the MOM scheme, which is the scheme used in our computations), and this indeed what happens. At this point the system is “tuned”, and one can construct and analyze other quantities that are built from  $\Delta$ ,  $F$  and  $g$ , as done in the next two sections.

**The  $G$  and  $L$  auxiliary functions.** The first quantities that can be studied by means of the procedure just described, are the auxiliary functions  $G$  and  $L$ , which in the Landau gauge one can prove to be related to the dressing function  $F(q^2)$  through the BRST identity [15]  $F^{-1}(q^2) = 1 + G(q^2) + L(q^2)$ . Since, under very general conditions on the gluon and ghost propagators,  $L(0) = 0$  one has the IR relation  $F^{-1}(0) = 1 + G(0)$ . Thus we see

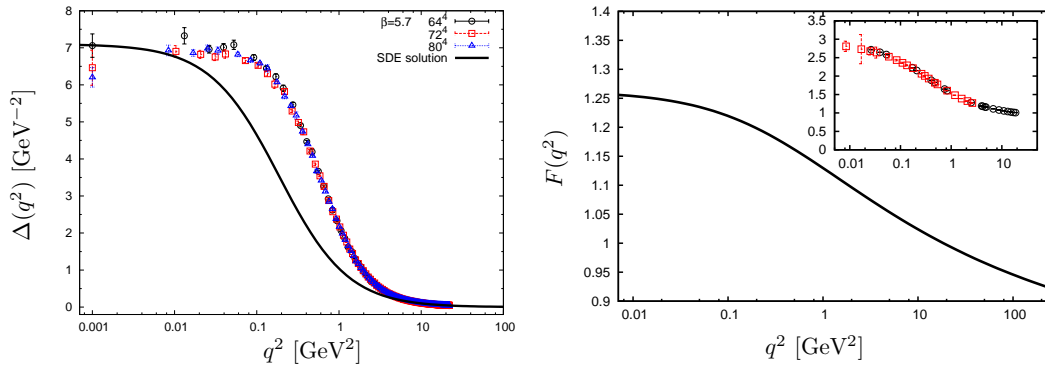


**FIGURE 3.** Gluon propagator and ghost dressing function for the SU(3) gauge group, and comparison with the corresponding lattice data of [9].

that a divergent (or *enhanced*) dressing function requires the condition  $G(0) = -1$ . The latter looks suspiciously similar to the Kugo-Ojima confinement criterion, demanding that a certain function  $u(q^2)$  (the Kugo-Ojima function) acquires the IR value  $u(0) = -1$ . Indeed, it is possible to show (in the Landau gauge only!) that  $G$  is nothing but the Kugo-Ojima function [15]:  $u(q^2) \equiv G(q^2)$ .

In Fig. (4) we show these auxiliary functions calculated at different renormalization points. One can see that indeed  $L(0) = 0$  and that in general  $L$  is suppressed with respect to  $G$ . In addition one finds that the function  $G$  saturates at an IR value bigger than  $-1$  (around  $-2/3$  for the renormalization points chosen) once again excluding IR enhancement of the ghost dressing function. Also these results are in good agreement with direct lattice calculations of the Kugo-Ojima function.

**The effective charge.** Another important information that can be extracted from the PT-BFM equations is the running of the QCD effective charge for a wide range of physical momenta, and, in particular, its behavior and value in the deep IR. The effective charge is invariant under the renormalization group (RG), and lies at the interface between perturbative and non-perturbative effects in QCD, providing a continuous interpolation between two physically distinct regimes: the deep UV, where perturbation theory is reliable, and the deep IR, where non-perturbative techniques must be employed.

There are two possible RG-invariant products on which a definition of the effective charge can be based, namely  $\hat{r}(q^2) = g^2(\mu^2)\Delta(q^2)F^2(q^2)$ , which exploits the non-renormalization property of the ghost vertex in the Landau gauge, and  $\hat{d}(q^2) = g^2(\mu^2)\hat{\Delta}(q^2)$ , which relies on the fact that in the background quantities satisfy Ward (as opposed to Slavnov-Taylor) identities. These two *dimensionful* quantities [mass dimension of  $-2$ ] share an important common ingredient, namely the scalar cofactor of the gluon propagator,  $\Delta(q^2)$ , which actually sets the scale. The next step is to extract a *dimensionless* quantity that would correspond to the non-perturbative effective charge. Perturbatively, i.e., for asymptotically large momenta, it is clear that the mass scale is saturated simply by  $q^2$ , the bare gluon propagator, and the effective charge is defined by pulling a  $q^{-2}$  out of the corresponding RG-invariant quantity. Of course, in the IR the gluon propagator becomes effectively massive; therefore, particular care is needed

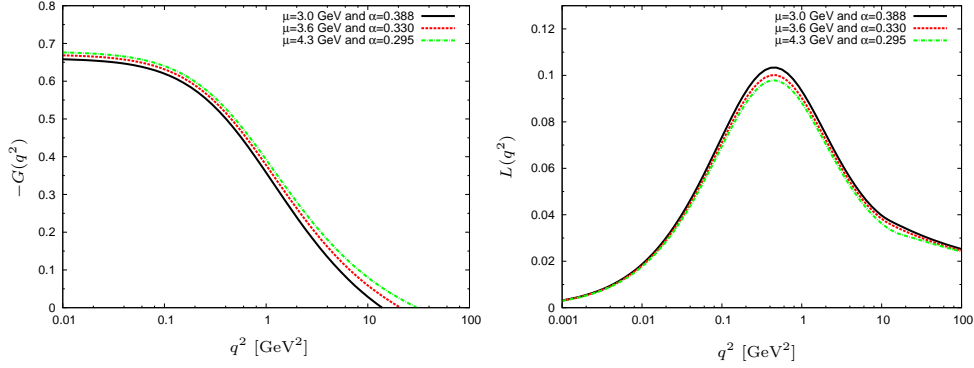


**FIGURE 4.** The form factors  $-G(q^2)$  and  $L(q^2)$  determined from Eq. (4.2) at different normalization points  $\mu$ , using the procedure specified in the text.

in deciding exactly what combination of mass scales ought to be pulled out. The correct procedure in such a case [5] is to pull out a massive propagator of the form (in the Euclidean space)  $[q^2 + m^2(q^2)]^{-1}$ , with  $m^2(q^2)$  the dynamical gluon mass. One has [16]

$$\alpha_{\text{gh}}(q^2) = \alpha(\mu^2)[q^2 + m^2(q^2)]\Delta(q^2)F^2(q^2), \quad \alpha(q^2) = \alpha(\mu^2)[q^2 + m^2(q^2)]\widehat{\Delta}(q^2), \quad (3)$$

and, due to the BRST identity between  $F$ ,  $G$  and  $L$ , the two effective charges are related:

$$\alpha(q^2) = \alpha_{\text{gh}}(q^2) \left[ 1 + \frac{L(q^2)}{1 + G(q^2)} \right]^2. \quad (4)$$

Since  $L(0) = 0$  we therefore see that not only the two effective charges coincide in the UV region where they should reproduce the perturbative result, but also in the deep IR where one has  $\alpha(0) = \alpha_{\text{gh}}(0)$ . In addition, due to the relative suppression of  $L$  as compared to  $G$ , even in the region of intermediate momenta, where the difference reaches its maximum, the relative difference between the two charges is small.

In Fig. 5 we show both a check of the RG-invariance of the combinations  $\widehat{r}$  and  $\widehat{d}$ , as well as a comparison between the effective charges (3) extracted from the lattice data for two different values of the running gluon mass.

## CONCLUSIONS

In this talk we have outlined the salient features of the SDEs formulated within the PT-BFM framework. A number of examples of the considerable potential offered by their interplay with the lattice simulations have also been given. Clearly, several aspects need to be further investigated, and in particular: (i) to improve the agreement between the PT-BFM and lattice results by devising better vertex Ansätze for implementing the Schwinger mechanism; (ii) to study on the lattice how the results change when calculations are performed in gauges other than the Landau; (iii) ideally, to code on the lattice the BFM in the Feynman gauge, along the lines suggested in [17], where a plethora of results are known to be free from gauge artifacts [12].

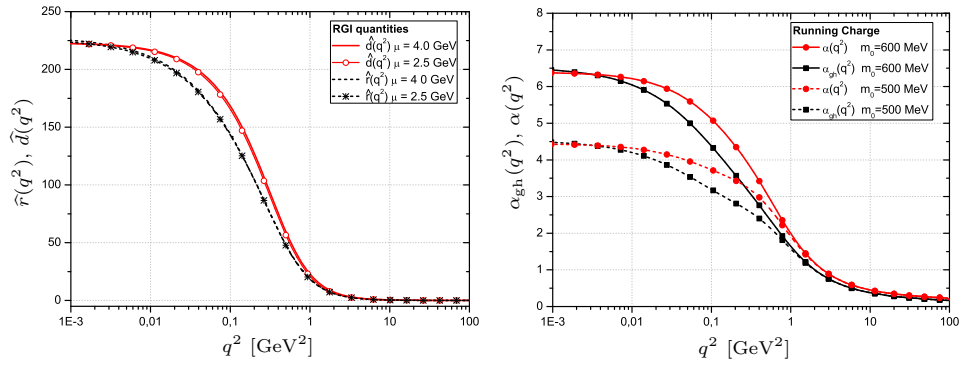


**FIGURE 5.** *Left panel:* Comparison between the two RG-invariant products  $\hat{d}(q^2)$  (solid line) and  $\hat{r}(q^2)$  (dashed line). *Right panel:* Comparison between the QCD effective charge extracted from lattice data:  $\alpha(q^2)$  (red line with circles) and  $\alpha_{\text{gh}}$  (black line with squares) for two different masses  $m_0$ .

## REFERENCES

1. For a thorough and concise review of the recent lattice literature on the topic see A. Cucchieri and T. Mendes, PoS **QCD-TNT09**, 026 (2009)
2. D. Binosi and J. Papavassiliou, Phys. Rev. D **77**, 061702(R) (2008); JHEP **0811**, 063 (2008).
3. P. Boucaud, J. P. Leroy, A. L. Yaouanc, J. Micheli, O. Pene and J. Rodriguez-Quintero, JHEP **0806**, 012 (2008).
4. A. C. Aguilar, D. Binosi and J. Papavassiliou, Phys. Rev. D **78**, 025010 (2008).
5. J. M. Cornwall, Phys. Rev. D **26**, 1453 (1982).
6. See C. S. Fischer, J. Phys. G **32**, R253 (2006), and references therein.
7. T. Kugo and I. Ojima, Prog. Theor. Phys. Suppl. **66**, 1 (1979).
8. V. N. Gribov, Nucl. Phys. B **139**, 1 (1978); D. Zwanziger, Nucl. Phys. B **364** (1991) 127.
9. I. L. Bogolubsky, E. M. Ilgenfritz, M. Muller-Preussker and A. Sternbeck, PoS **LAT2007**, 290 (2007).
10. A. Cucchieri and T. Mendes, PoS **LAT2007**, 297 (2007).
11. D. Dudal, J. A. Gracey, S. P. Sorella, N. Vandersickel and H. Verschelde, Phys. Rev. D **78**, 065047 (2008).
12. J. M. Cornwall and J. Papavassiliou, Phys. Rev. D **40**, 3474 (1989); D. Binosi and J. Papavassiliou, Phys. Rev. D **66**(R), 111901 (2002); J. Phys. G **30**, 203 (2004); D. Binosi and J. Papavassiliou, Phys. Rept. **479**, 1 (2009).
13. P. A. Grassi, T. Hurth and M. Steinhauser, Annals Phys. **288**, 197 (2001); D. Binosi and J. Papavassiliou, Phys. Rev. D **66**, 025024 (2002).
14. J. S. Schwinger, Phys. Rev. **125**, 397-398 (1962); Phys. Rev. **128**, 2425-2429 (1962).
15. T. Kugo, arXiv:hep-th/9511033; P. A. Grassi, T. Hurth and A. Quadri, Phys. Rev. D **70**, 105014 (2004); A. C. Aguilar, D. Binosi and J. Papavassiliou, JHEP **0911**, 066 (2009).
16. A. C. Aguilar, D. Binosi and J. Papavassiliou, PoS **LC2008**, 050 (2008); JHEP **1007**, 002 (2010); A. C. Aguilar, D. Binosi, J. Papavassiliou and J. Rodriguez-Quintero, Phys. Rev. D **80**, 085018 (2009).
17. R. F. Dashen and D. J. Gross, Phys. Rev. D **23**, 2340 (1981).